ARCHIVES OF ELECTRICAL ENGINEERING VOL. 66(4), pp. 717-730 (2017)

DOI 10.1515/aee-2017-0054

Comparison of transformer modeling on riser pole arresters behavior during switching transients

AMIR ABBASZADEH, MEHRDAD ABEDI, ALI DOUSTMOHAMMADI

Amirkabir University of Technology Department of Electrical Engineering
424 Hafez Ave, Tehran, Iran
e-mail: amir.abbaszadeh@aut.ac.ir

(Received: 08.03.2017, revised: 16.06.2017)

Abstract: Arresters are widely used in power systems to protect other equipment against overvoltages. However, in some conditions, they can't operate successfully. One of the disturbances leading to the failure of the riser pole arresters is the ferroresonance overvoltages. In this paper, at first the influence of different transformer simulation models of ATP software on the occurrence of ferroresonance is studied and then the effect of ferroresonance on the riser pole arrester has been scrutinized through the thermal and electrical performance of the arrester in an underground distribution system. The results show that the arrester temperature rises due to energy dissipation in a ferroresonance circumstance, which indeed may result into the explosion of the arrester. Also, applying different models of the transformer in the ATP software and comparing the results, it is shown that the available models do not show the same effect on the arrester.

Key words: arresters, ATP software, ferroresonance, transformer, power system transients

1. Introduction

With the increasing use of cable line and low-loss transformers, the probability of ferroresonance occurrence has increased. This phenomenon happens when a lightly loaded transformer, fed by a cable line, is subjected to either a single or a two-phase switching, especially in power system restoration situations where a specific amount of load should be picked-up. There are several records of ferroresonance and its effect on the power system equipment [1-4]. Ferroresonance is a type of resonance which occurs when a circuit containing a nonlinear inductance is energized by a source and a capacitor in series [5]. Linear resonance and ferroresonance are not similar. The resonance is a frequency dependent phenomenon within which current and voltage are linearly related to each other. However, during ferroresonance condition, due to the system operating point variations, sudden jumps of the voltage and cur-

rent will occur. The relationship between the voltage and current in this phenomenon is dependent not only on the frequency but also on other parameters such as the magnitude of voltage, the remaining magnetic flux and the initial condition of the transformer core [6].

In [7], distribution circuit ferroresonance has been recognized to be one of the main causes of arrester failure. However, in [8] it has been concluded that ferroresonance overvoltages may not be so severe and arresters may operate successfully. In [9] an analysis is done to explore the cause of the explosion of the arresters. In [10] the T and π models of a transformer are compared with each other along with the experimental results. Viena and his colleagues have studied different models of two transformers in the ATP software and their effect on the occurrence of ferroresonance, but they did not analyze the electrical and the thermal behavior of arresters during the ferroresonance condition [11]. It is worth to be noted that, during the primary stages of power restoration, lightly loaded distribution transformers should be energized to pick-up some load for the stability of the black-start unit. In this case, unexpected overvoltages may occur due to nonlinear characteristics of power system equipment which may damage them [12]. The goal of the present paper is to study the effect of the transformer model on the riser pole arresters from the electrical and the thermal behavior point of view in ferroresonance condition. Doing so the operators of distribution control centers can predict whether the switching of a lightly load transformer will result into ferroresonance condition or not, while in the former case they can change the configuration of the distribution system Therefore the safety of the equipment of power systems can be maintained.

2. Transformer modeling in ATP software

The behavior of the transformer depends on the frequency in the study. In the high-frequency condition, the performance of the transformer is specified by the capacitance of the windings. However, in the low or medium frequency conditions, the magnetic couplings between windings and saturation of the core [13] determine the behavior of the transformer. Basically the frequency of ferroresonance is in the medium and low range therefore the saturation of the core is of importance in this particular case.

In order to study the effect of the transformer model on the ferroresonance phenomenon, three different models, proposed in the ATP software, are explained briefly in the following sections.

2.1. BCTRAN model

This model is used to represent the shell or core-type transformer, with any number of windings; it is also suitable for both three and single-phase transformers. Parameters needed for this model are estimated by applying short circuit and open circuit tests. Two different matrices are used in this model: Matrix [$\boldsymbol{A}$] which is the inverse of the inductance [$\boldsymbol{L}$] matrix, [$\boldsymbol{r}$] which is related to the resistance of the windings. W is the nominal angular frequency. It is impossible to directly implement the nonlinear behavior of the transformer, i.e. saturation and hysteresis, to this model. Also, in order to simulate the nonlinearity, an external magnetizing

branch can be connected to the transformer terminals. This will provide the ability to consider the initial flux of the core. Taking topology into account, connecting an external branch to the transformer terminal may lead to inaccuracy.

2.2. SATURABLE model

This model is to represent the single-phase and three-phase circuit of the transformer. Nonlinearities such as saturation and hysteresis are modeled by considering a nonlinear inductance, connected to wye-point of the transformer. The following parameters need to be estimated for this model: the resistance and the inductance of each branch, the transformation ratio and information about the magnetizing branch. The numerical instability may occur while applying this model for representing three winding transformer, which is primarily due to topological concerns.

2.3. XFMR model

This model has been recently introduced, and it is also considered as a hybrid transformer model [14]. Similar to the BCTRAN model, this model utilizes the matrix representation. For demonstrating the magnetic model of the core in yokes and legs of the transformer, the fundamentals of duality are used. Although this model is one of the strongest models, the complexity and the amount of its data have resulted in its limited application in the scientific community. The information needed for this model can be estimated from three different sources: a) design information; b) manufacturing data test; c) typical data based on nominal voltage and power.

The main problem of this model is tuning the parameters of the Ferrolich equation which simulates the *B-H* behavior of the core materials. In order to determine the Ferrolich equation, μ_m, i.e. the maximum relative permeability of the core, and the β_{sat}, i.e. the density of flux for the maximum saturation, are needed which can be obtained in the following manner:

$$\mu = \frac{\mathrm{d}B}{\mathrm{d}H}, \tag{1}$$

$$B = \frac{H}{c + bH}. \tag{2}$$

The values of constants b and c can be obtained from the core material. Considering (1) and (2), the permeability can be stated:

$$\mu = \frac{(1 - bB)^2}{c}. \tag{3}$$

As the flux density reaches to its maximum, the relative permeability becomes one. Utilizing this fact, the relation between b and c can be found. Setting β equal to zero reduces (3) to:

$$c = \frac{1}{\mu_0 \mu_m}. \tag{4}$$

When the value of constant c is known and β is equal to β_{sat}, the value of constant b is:

$$b = \frac{1-(1/\sqrt{\mu_m})}{\beta_{sat}}. \tag{5}$$

By determining the constants b and c, the Ferrolich equation illustrates the B-H curve in the ranges between $\beta = 0$ and $\beta = \beta_{sat}$ [11].

3. Riser pole arresters

Riser pole arrester is an arrester for pole mounting; it is normally used to protect underground distribution cables and equipment. The definition of this type of arrester does not exist in IEC. It is worthy to be noted that in the IEEE definition, it is a type of arrester and not a class of arresters; furthermore, there are no special tests prescribed in the IEEE standard.

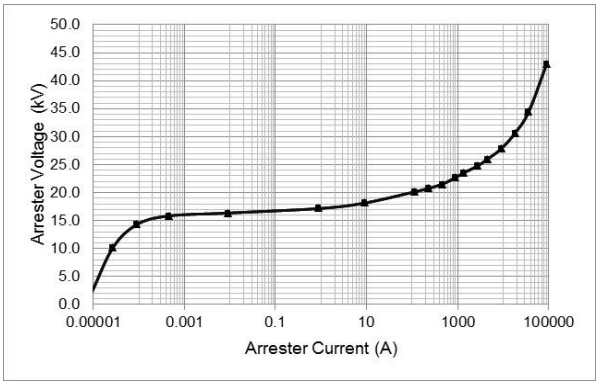

Fig. 1. The *V-I* characteristic of the arrester

It is due to the fact that the capacitance of the system is quite high in the underground circuits compared with the overhead circuits that special arresters at the riser pole are utilized. As a result of the well-known phenomenon of traveling wave reflections, it is very likely that the amplitude of voltage doubles at some point in the underground portion of the line. The *V-I* characteristics of the arrester used in the simulations is plotted in Fig. 1. Also the arrester data for calculation the energy dissipation amount and temperature rise value are provided in Tab 1.

Table 1. Arrester's data

Manufacture	**GE**
U_r	10 (kV)
U_c	8.4 (kV)
H	175 (mm)
MOV disk diameter	30 (mm)

Where U_r is the rated voltage and U_c is the maximum continuous operating voltage and H is the overall height of the arrester. Based on the data and the formulation given below the thermal behavior of the arrester is monitored.

$$\Delta T = \frac{E}{M \times SH}, \tag{6}$$

where T is the temperature in °C, E is the energy absorbed during the surge in J. The amount of energy depends on the current, voltage of the surge and the duration of it. M is the mass of the MOV disk in g. SH is the heat which needed to raise the temperature of the unit mass of a specific substance by 1°C in J/g/°C. The value of specific heat for the MOV arrester is assumed 0.55 [15]. If the mass of the MOV disk is not available, the equation of volume can be used as:

$$M = V \times D, \tag{7}$$

where V is the volume of the material in cm3. D is the density of the material in g/cm3 and it is considered to be 5.35.

4. Simulation results

In this section, first, the configuration of the tested system is introduced. Then the ferroresonance is simulated and the effect of different models of the transformer is studied. Furthermore, a riser pole arrester is installed on the considered system to survey the effect of ferroresonance on this type of arrester. Test system is a real part of a distribution system widely used for industrial and household consumption. The graphical representation of the system is depicted in Fig. 2. It should be noted that the test system and the two different transformers which are used for this study are the same as in [11].

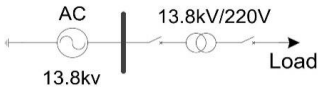

Fig. 2. The single-line diagram (SLD) of test system

4.1. Ferroresonance simulation in different cases

In all cases, single switching is applied. It means that phase A will be opened and the other two phases remain closed. In this paper, two types of transformers, i.e. 75 kVA and 500 kVA, with several different cable lengths (L), i.e. 100, 150, 200, 250 and 300 m, are considered. It is to be noted that, the cases with the cable lengths of 100 and 300 m are selected to study the ferroresonance effect on the arrester. Therefore the case studies related to cable lengths of 150, 200 and 250 m are brought altogether in section 4.1.6. Due to the lack of geometric data for the 500 kVA transformer, the XFMR model of this transformer is not included in the case studies. It is necessary to emphasize that related results for the ferroresonance phenomenon have also been reported in [11]. Nevertheless, in the present paper, the ferroresonance effect

on the arrester is studied. It is worth to be noted that other configurations which result into ferroresonance occurrence can also be considered for the case studies in future works.

4.1.1. Case1: simulation of the 75 kVA transformer by the BCTRAN model

As plotted in Fig. 3, when the length of cable is 100 m, the ferroresonance does not occur. Nonetheless, it occurs for the cable with the length of 300 m. whereas switching of two phases leads to ferroresonance for the cable with the length of 100 m.

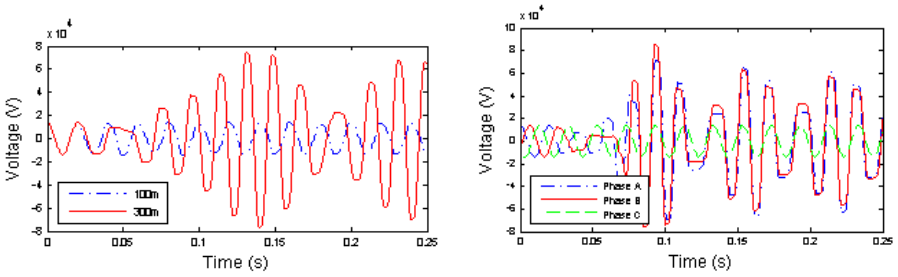

(a) (b)

Fig. 3. Ferroresonance simulation for 100 m and 300 m cable lengths (a), switching of two phases for the cable with the length of 100 m (b)

4.1.2. Case2: simulation of the 75 kVA transformer by the XFMR model

In this case, again phase A is opened and the other two phases remain closed. As it can be seen in Fig. 4, the ferroresonance occurs for both cable lengths.

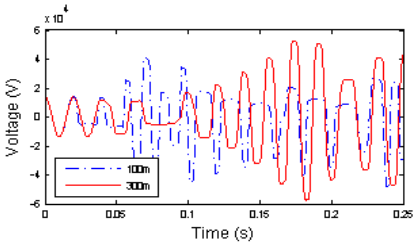

Fig. 4. Ferroresonance simulation for the 100 and 300 m cable lengths

4.1.3. Simulation of the 75 kVA transformer by the SATURABLE model

In this case, the SATURABLE model of the transformer is applied as plotted in Fig. 5.

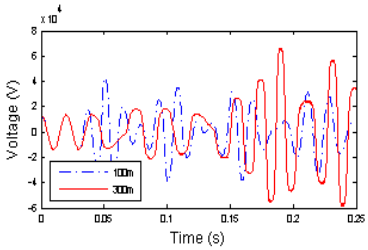

Fig. 5. Ferroresonance simulation for the 100 and 300 m cable lengths

4.1.4. Simulation of the 500 kVA transformer by the BCTRAN model

Fig. 6, shows the voltage of phase A at the primary side of the 500 kVA transformer for two different cable lengths using the BCTRAN model.

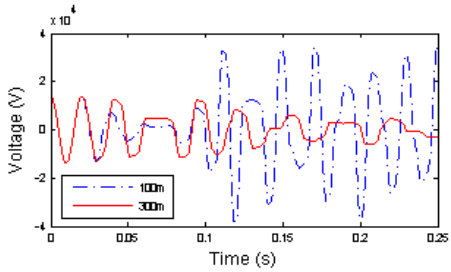

Fig. 6. Ferroresonance simulation for the 100 and 300 m cable lengths

4.1.5. Simulation of the 500 kVA transformer by the SATURABLE model

The voltage of phase A at the primary side of the 500 kVA transformer is plotted in Fig. 7, for two different cable lengths.

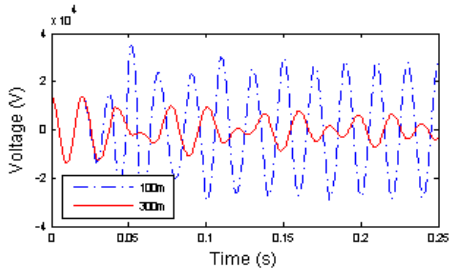

Fig. 7. Ferroresonance simulation for the 100 and 300 m cable lengths

4.1.6. Analysing the effect of different cable lengths on ferroresonance

In this section three different cable lengths, i.e. 150, 200 and 250 m are simulated for each of transformer models and the results are brought in related pictures. It is worth to be noted that for better comparison, the maximum voltage of all the investigated cases are provided in Table 2.

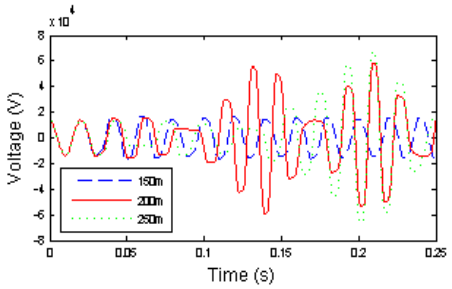

Fig. 8. Ferroresonance simulation for the 150, 200 and 250 m cable lengths considering BCTRAN model of the 75 kVA transformer

Based on the above mentioned explanations for the BCTRAN model of the 75 kVA transformer three different cable lengths are investigated and as Fig. 8, shows the ferroresonance does not occur for the cable length of 150 m, although for the cable lengths of 200 and 250 this phenomenon happens. It is to be noted that the maximum ferroresonance voltage is in direct relation with the cable length.

Fig. 9, illustrates the voltage curves for the 75 kVA transformer considering XFMR model. As it can be deducted from this picture ferroresonance occurs for all the cable lengths.

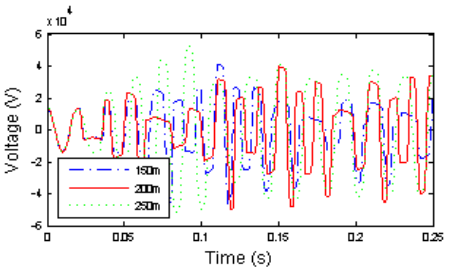

Fig. 9. Ferroresonance simulation for the 150, 200 and 250 m cable lengths considering XFMR model of the 75 kVA transformer

The same simulations are done for the 75 kVA transformer considering the SATURABLE model of the transformer. As it can be concluded from Fig. 10, the ferroresonance occurs for the 150 and 200 m cable lengths.

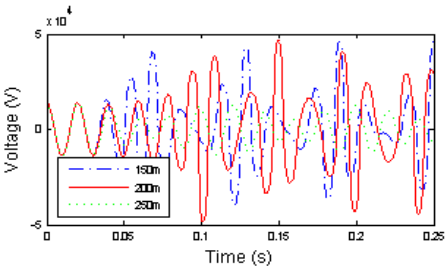

Fig. 10. Ferroresonance simulation for the 150, 200 and 250 m cable lengths considering the SATURABLE model of the 75 kVA transformer

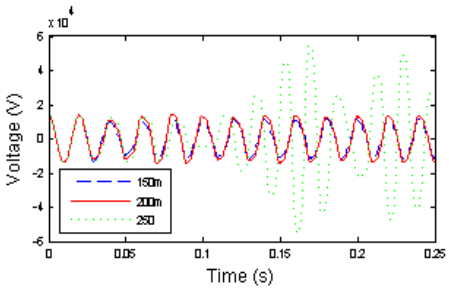

Fig. 11. Ferroresonance simulation for the 150, 200 and 250 m cable lengths considering the BCTRAN model of the 500 kVA transformer

These simulations are repeated for the 500 kVA transformer considering the BCTRAN and SATURABLE model of the transformer. As it can be noticed form Fig. 11, in the case where

the BCTRAN transformer model is considered, the 250 m cable length causes the ferroresonance to happen.

In the next simulations the SATURABLE model of the 500 kVA transformer is considered where the cable length varies from 150 to 250 m by a span of 50 m. As it is illustrated in Fig. 12, the ferroresonance does not occur for the cable with the length of 250 m.

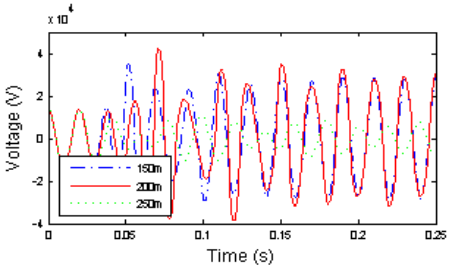

Fig. 12. Ferroresonance simulation for the 150, 200 and 250 m cable lengths considering the SATURABLE model of the 500 kVA transformer

In order to have a better comparison, the maximum of voltage for different cable lengths are demonstrated in Table 2.

Table 2. Detailed information of maximum of voltages for different transformer models

Transformer capacity	**75 kVA**			**500kVA**		
Cable length	150 m	200 m	250 m	150 m	200 m	250 m
BCTRAN	16.882 (kV)	58.678 (kV)	67.64 (kV)	13.80 (kV)	14.613 (kV)	55.378 (kV)
SATURABLE	46.348 (kV)	46.869 (kV)	13.89 (kV)	42.294 (kV)	47.756 (kV)	13.803 (kV)
XFMR	40.855 (kV)	39.776 (kV)	52.74 (kV)	No available data		

4.2. The effect of Ferroresonance on the arrester

In this section, an arrester is installed and the effect of ferroresonance is surveyed. In addition, the energy absorption and the temperature rise in the arrester are monitored. The single line diagram of the system is shown in Fig. 13, where an arrester is considered in the test system.

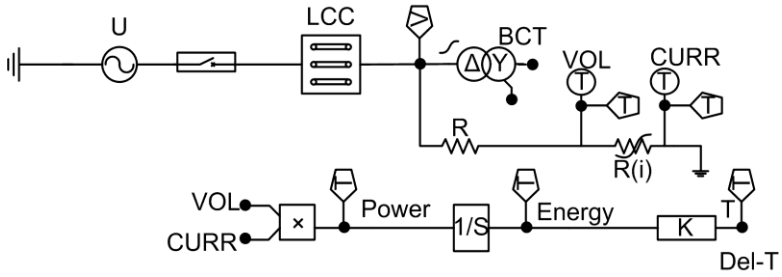

Fig. 13. The SLD of the test system equipped with arrester in the ATP software

4.2.1. The 75 kVA transformer and the BCTRAN model with arrester

The voltage of phase A, alongside the voltage of the other two phases, at the primary side of the transformer in the presence of the arrester is plotted in Fig. 14. Also the temperature rise and energy absorption of the arrester are shown in this figure.

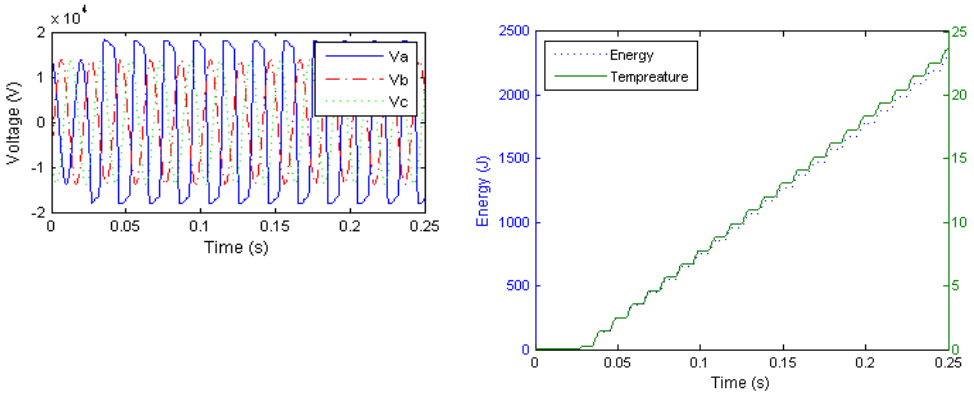

(a) (b)

Fig. 14. Arrester operation in ferroresonance condition for the cable length of 300 m: (a) temperature rise; (b) energy absorption of the arrester

4.2.2. The 75 kVA transformer and XFMR model with arrester

The same method of analysis is applied to the 75 kVA transformer using the XFMR model. In Figs. 15 and 16, the arrester operation; its temperature and the energy absorption for both cable lengths are plotted.

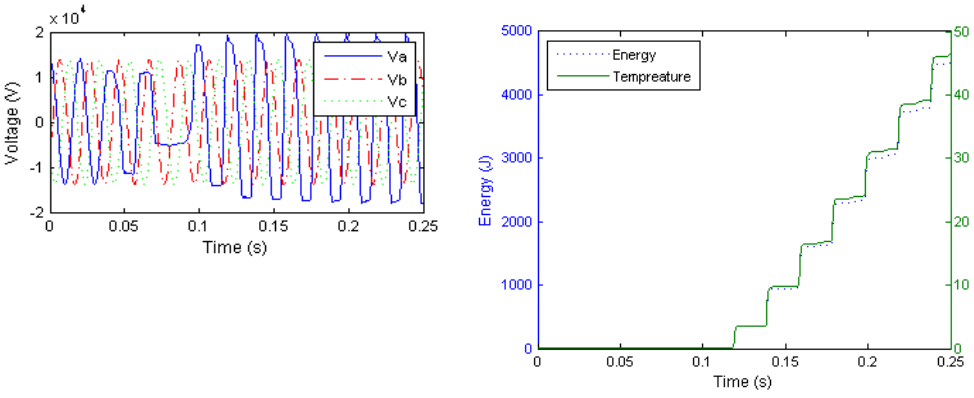

(a) (b)

Fig. 15. Arrester operation during ferroresonance condition for the cable length of 300 m: (a) temperature rise; (b) energy absorption of the arrester

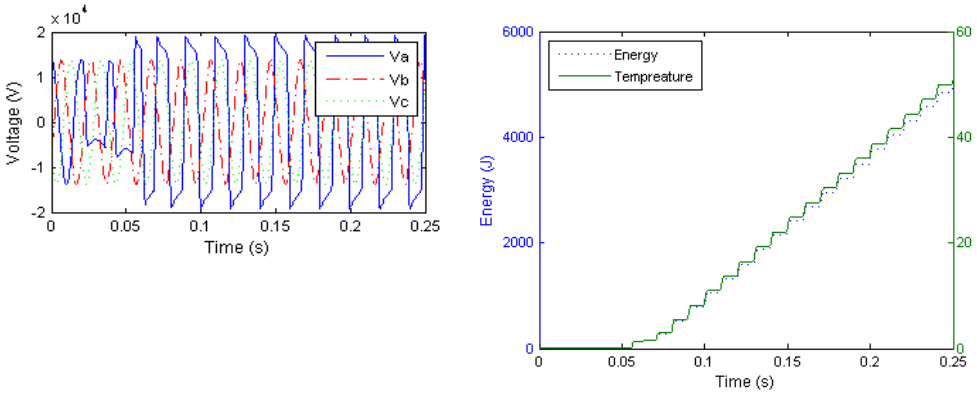

(a) (b)

Fig. 16. Arrester operation during ferroresonance condition for the cable length of 100 m: (a) temperature rise; (b) energy absorption of the arrester

4.2.3. The 75 kVA transformer and the SATURABLE model with arrester

This case is studied applying the SATURABLE model of the transformer, and the results are plotted in Figs. 17 and 18.

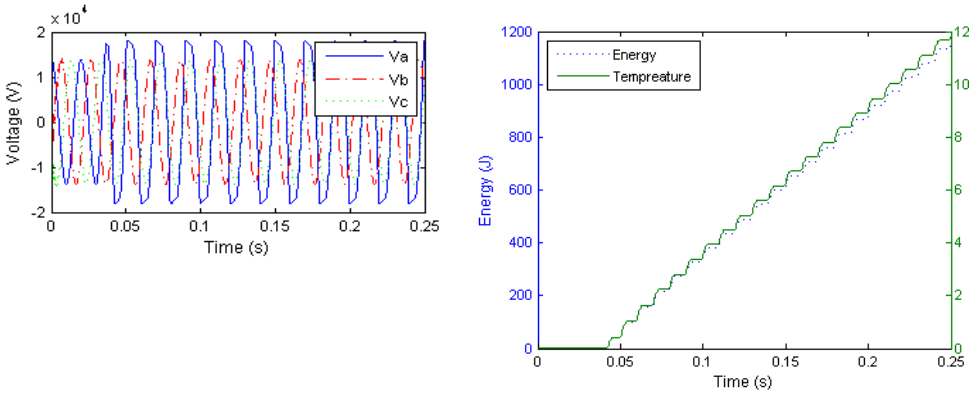

(a) (b)

Fig. 17. Arrester operation during ferroresonance condition for the cable length of 100 m: (a) temperature rise; (b) energy absorption of the arrester

4.2.4. The 500 kVA transformer and the BCTRAN model with the arrester

In this section, the same analysis is conducted for the 500 kVA transformer and the results are depicted in Fig. 19. In this case, the BCTRAN model of 500 kVA transformer is applied and the performance of the arrester is plotted. It should be noted that for the cable with the length of 300 m, ferroresonance did not occur.

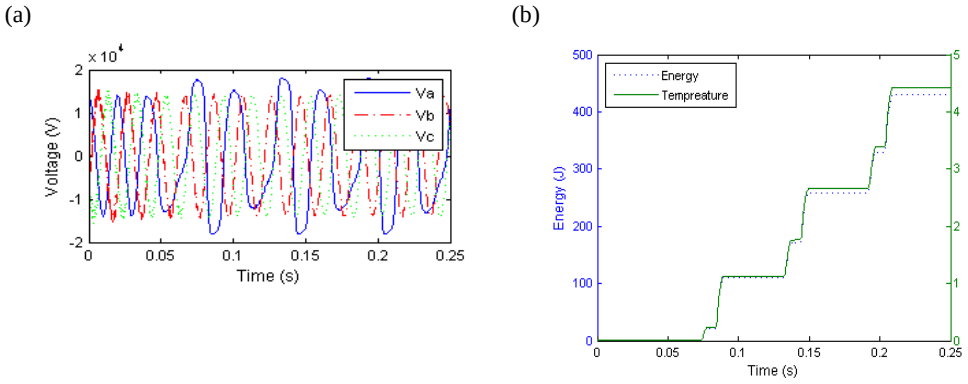

Fig. 18. Arrester operation during ferroresonance condition for the cable length of 300 m: (a) temperature rise; (b) energy absorption of the arrester

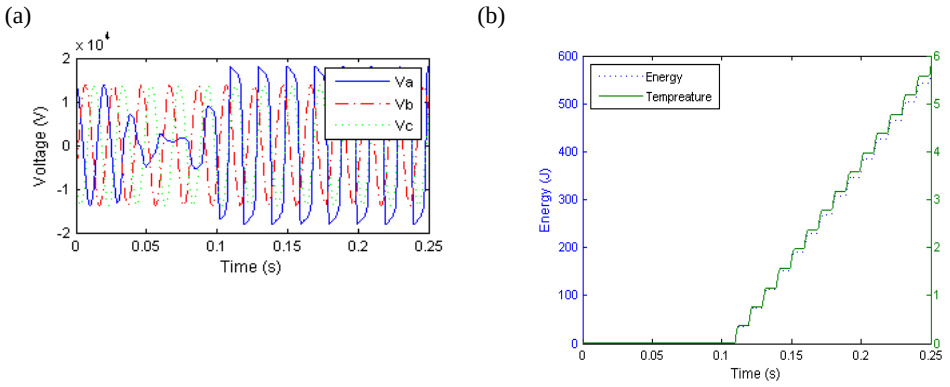

Fig. 19. Arrester operation during ferroresonance condition for the cable length of 100 m: (a) temperature rise; (b) energy absorption of the arrester

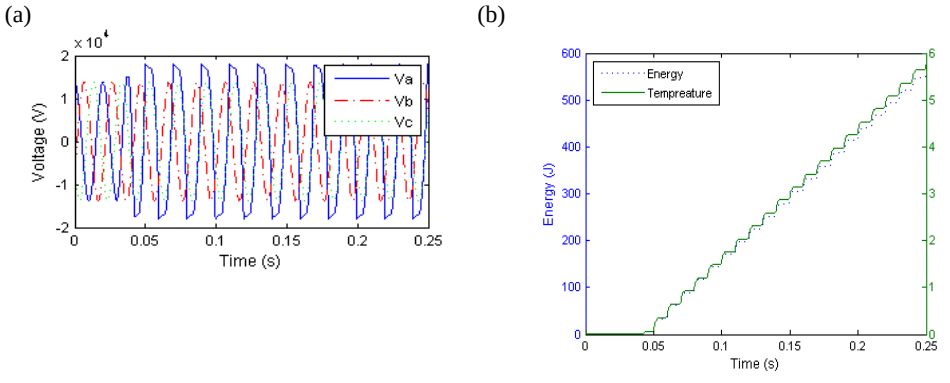

Fig. 20. Arrester operation for the cable length of 100 m: (a) temperature rise;(b) energy absorption of the arrester

4.2.5. The SATURABLE model of the 500 kVA transformer with arrester

For the SATURABLE model of 500 kVA transformer, the results are plotted in Fig. 20. For better comparison, the details of all the investigated cases are provided in Table 3.

Table 3. Further information

Case	75 kVA transformer			Case	500 kVA transformer	
	XFMR	BCTRAN	SATURABLE		BCTRAN	SATURABLE
Max voltage (kV) 100 (m)	48.19	Negligible	43.022	Max voltage (kV), 100 (m)	34.4	35.099
Energy (J) 100 (m)	4940.4	Negligible	1146.2	Energy (J) 100 (m)	559.779	557.311
Temperature (°C) 100 (m)	50.88	Negligible	11.8059	Temperature (°C) 100 (m)	5.7657	5.7403
Max voltage (kV) 300 (m)	57.36	74.96	66.095	Max voltage (kV) 300 (m)	Ferroresonance did not ocurr	
Energy (J) 300 (m)	4510.9	2248.5	430.018	Energy (J) 300 (m)		
Temperature (°C) 300 (m)	46.461	23.83	4.4292	Temperature (°C) 300 (m)		

5. Conclusions and future work

In this paper, first, the occurrence of the ferroresonance for the two different transformers with several cable lengths has been analyzed. It has been shown that ferroresonance is dependent on many factors, including the cable length, the transformer and its model. Also it can be deducted from the result that different simulation models of the transformer show diverse results regarding ferroresonance and lead to different levels of voltage. In the next step, the effect of the ferroresonance has been analyzed on the riser pole arrester for the cables with the length of 100 and 300 m. This analysis would help the operators of distribution control centers predict whether the switching of a lightly load transformer will result into ferroresonance condition or not, especially in the restorative phase of the power system. As it has been shown in the results, the temperature rise and energy absorption of the riser pole arrester are different in the case of applying different simulation models of the transformer in ferroresonance condition. For the 500 kVA transformer results are in consistent with each other, whereas for the 75 kVA transformer they are not in compliance with each other. Therefore writers suggest that same analyses considering distribution transformers with different rated power, manufacturer and models besides the one utilized in this article can be executed in future work. Also field tests can be done to demonstrate the degree of validity of different transformer models.

Acknowledgements

Writer would like to thank reviewers for their useful comments and the Iran Grid Management Company (IGMC) for their data support during the preparation of this paper.

References

[1] Bohmann L.J., McDaniel J., Stanek E.K., *Lightning arrester failure and ferroresonance on a distribution system*, IEEE Transactions on Industry Applications. vol. 29, no. 6, pp. 1189-1195 (1993).

[2] Walling R.A., Hartana R.K., Reckard R.M., Sampat M.P., Balgie T.R., *Performance of* metal-*oxide arresters exposed to ferroresonance in padmount transformers*, IEEE Transactions on Power Delivery, vol. 9, no. 2, pp. 788-795 (1993).

[3] Dugan R.C., *Examples of ferroresonance in distribution systems*, IEEE Power Engineering Society General Meeting, Toronto, Canada, pp. 1213-1215 (2003).

[4] MacPhee A., McKee S., Simpson R., *Ferroresonance in electrical systems*, COMPEL, The International Journal For Computation And Mathematics In Electrical and Electronic Engineering, vol. 21, no. 2, pp. 265-273 (2004).

[5] Dugan R.C., McGranaghan M.F., Beaty H.W., Santoso S., *Electrical power systems quality*, McGraw-Hill company (2003).

[6] Valverde V., Zamora I., Buigues G., Mazon A.J., *Ferroresonance in voltage transformers: Analysis and simulations*, International Conference on Renewable Energies and Power Quality (ICREPQ"07), Sevilla, Spain, pp. 465-471 (2007).

[7] Sakshaug E., Burke J., Kresge J., *Metal oxide arresters on distribution systems: fundamental considerations*, IEEE Transactions on Power Delivery, vol. 4, no. 4, pp. 2076-2089 (1989).

[8] Short T., Burke J., Mancao R.T., *Application of MOVs in the distribution environment*, IEEE Transactions on Power Delivery, vol. 9, no. 1, pp. 293-305 (1994).

[9] Pattanapakdee K., Banmongkol C., *Failure of riser pole arrester due to station service transformer ferroresonance*, International Conference on Power Systems Transients (IPST), Lyon, France (2007).

[10] Jazebi S., Farazmand A., Murali P., *A Comparative Study on π and T Equivalent Models for the Analysis of Transformer Ferroresonance*, IEEE Transactions on Power Delivery, 2013, vol. 1, no. 28 pp. 526-528 (2013).

[11] Viena L., Moreira A., Ferreira R., de Castro A., de Jesus N., *Analysis and application of transformer models in the ATP program for the* study *of ferroresonance*, Transmission and Distribution Conference and Exposition: Latin America (T&D-LA), pp. 738-743 (2010).

[12] Sadeghkhani I., Ketabi A., Feuillet R., *An approach to evaluate switching overvoltages during power system restoratin*, Serbian Journal of Electrical Engineering, vol. 9, no. 2, pp. 171-187 (2012).

[13] Mork B., Gonzalez F., Ishchenko D., *Hybrid transformer model for transient simulation – Part I: Development and parameters*, IEEE Transactions on Power Delivery, vol. 22, no. 1, pp. 248-255 (2007).

[14] Prikler L., Høidalen H.K., *ATPDraw version 3.5 for Windows 9x/NT/2000/XP User's Manual*, Sinef Energy Research (2002).

[15] www.arresterworks.com, accessed November 2016.